Colloid & Polymer Science Colloid Polym Sci 272:467–477 (1994)

The kinetics of poly(*N*-isopropylacrylamide) microgel latex formation

X. Wu, R. H. Pelton, A. E. Hamielec, D. R. Woods, and W. McPhee

McMaster Centre for Pulp and Paper Research, Department of Chemical Engineering, McMaster University, Hamilton, Canada

Abstract: Conversion versus time curves were measured for poly(*N*-isopropylacrylamide) microgel latexes prepared by polymerization in water with sodium dodecyl sulfate, SDS. Polymerization rates increased with temperature with methylenebisacrylamide crosslinking monomer consumed faster than *N*-isopropylacrylamide. The particle diameter decreased with increasing concentrations of SDS in the polymerization recipe and there was evidence that the rate of polymerization increased somewhat with SDS concentration. Particle formation occurred by homogeneous nucleation as micelles were absent.

Comparison of particle size distributions from dynamic light scattering to those from a centrifugal sizer led to the conclusion that larger particles within a specific latex were less swollen with acetonitrile than were the smaller ones. This was interpreted as evidence for the polymer in larger particles having a higher crosslink density. Particle swelling was estimated from swelling ratios defined as the particle volume at 25 °C divided by the volume at 50 °C. In the absence of crosslinking poly(*N*-isopropylacrylamide) linear chains would dissolve at 25 °C. The swelling results indicated that the average crosslink density in the particles decreased with conversion. This was explained by the observation that the methylenebisacrylamide was consumed more quickly and is typical of crosslinking in emulsion polymerization where polymer particles have high polymer concentrations at their birth.

Key words: *N*-isopropylacrylamide polymerization – nucleation mechanisms – polymerization kinetics – gel swelling

Introduction

Surfactant-free, water swollen latexes based on poly(*N*-isopropylacrylamide) [1], (polyNIPAM) were first prepared in our laboratory [2–4]. Papers have been published describing latex preparation [2], electrokinetic properties [3], colloidal stability, and interactions of the particles with sodium dodecyl sulfate (SDS) [4]. The unique feature of polyNIPAM microgel latexes is that swelling with water and all related properties are very sensitive to temperature. For example, between room temperature and 40 °C the latex particle volume decreases by a factor of ten [3, 4]. Work from other laboratories on these fascinating particles is beginning to appear in the literature [5]. The purpose of this paper is to describe the first reported kinetic information about polyNIPAM latex formation.

The fundamental requirement for the formation of polyNIPAM latex is that the polymerization in water be conducted above 32 °C, the cloud point temperature (CPT) of polyNIPAM. Under these conditions the water soluble *N*-isopropylacrylamide, NIPAM, monomer reacts to give insoluble polymer. Colloidal stability studies have shown that below the CPT the particles are stabilized by three factors: 1) the chains on the exterior of the particles act as a steric stabilizer; 2) sulfate groups from the initiator and SDS give electrostatic stabilization, and 3) the van der Waal's attraction between the highly swollen particles will be low. By contrast, above the CPT only electrostatic forces stabilize the latex.

Experimental

NIPAM (Kodak) was purified by re-crystallization from toluene, hexane mixtures. Methylenebisacrylamide, BA was recrystallized from methanol. Potassium persulfate, KPS, (BDH, analytical grade) and SDS (Aldrich) were used without further purification.

Most of the preparations were conducted in a 1-L glass polymerization reactor fitted with a condenser, a glass stirring rod with a Teflon paddle, a reflux condenser and a nitrogen bubbling tube. The reactor was immersed in a water bath set at 50° or 70 °C. In a typical experiment 470 ml Milli Q water (Millipore Corp.), 7 g NIPAM, 0.7 g BA and 0.094 g SDS were added to the reactor. The solution was stirred at 200 RPM for 30 min with a nitrogen purge to remove oxygen. 0.28 g KPS dissolved in 30 mL water were added and the reaction was stirred for 4 h. Table 1 summarizes the latex recipes.

Samples taken during the reaction for kinetic measurements were quenched with methyl hydroquinone. Latexes were purified to remove SDS and other impurities by four successive centrifugations (Beckman L7 Ultracentrifuge, 10000 to 50000 RPM for 60 min.), decantations and dispersions in Milli Q water. The conductivity of the fourth supernatant liquid was typically 2 μS/cm.

Particle size and particle size distributions of the latexes were measured by dynamic light scattering with a NICOMP 370 autodilute Submicron Particle Sizer. Sizes and size distributions were computed by Version 10.3 of the NICOMP software using Gaussian Analysis. Volume weighted averages are presented herein however the intensity average diameters were similar (see Fig. 12). For most size measurements, the latex taken from the reactor was diluted approximately by 1000 with Milli-Q water.

A few particle size distributions were determined with a Horiba CAPA 700 which is a centrifugal particle size apparatus. The measurements were made in acetonitrile. The disk was accelerated at a rate of 960 RPM/min to a maximum of 10000 RPM.

Monomer conversion was measured by HPLC with an apparatus fitted with a LC-CN column (Supelco, Inc.), a 160 UV-Vis detector (Beckman Instruments) and a SP4200 integrator (Spectra-Physics). Milli-Q water was used as the mobile phase. Reported values are the average of at least three determinations with standard deviations less than 1 percent. Reaction rates were calculated from the slopes of straight line segments between consecutive conversion data on conversion versus time plots. On the basis of the standard deviation of the conversion measurements, the error in the rate data was estimated to be less than $\pm$ 5%.

Table 1. Recipes for latex polymerizations. The NIPAM concentration was 123.7 mmol/L, and the KPS concentration was 2.07 mmol/L

Designation	[BA] mmol/L	[SDS] mmol/L	T(°C)
LS1	9.08	0.409	70
LS6	9.08	0.409	50
LS8	0	0.409	70
LS9	9.08	0.409	70
LS10	9.08	2.460	70
5–76	9.08	0.728	70
5–72	9.08	2.00	70
5–77	9.08	0.208	70
5–70	9.08	4.00	70
5–78	18.2	0.65	70

Number concentrations of latex particles were difficult to determine because of the problems associated with measuring the absolute concentration of water in the latex particles. A viscosity method was based on the following relationship between ϕ, the volume fraction of particles, N_p and D, the corresponding number concentration and diameter (assuming a monodisperse particle size distribution).

$$6\phi = N_p D^3 \pi \,. \tag{1}$$

The volume fractions were estimated from experimental measurements of the reduced viscosity, η_r, using the expression given by Thomas [6].

$$\eta_r = 1 + 2.5\,\phi + 10.05\,\phi^2 + 0.00273\exp(16.6\,\phi) \tag{2}$$

Reduced viscosities were measured with a #75 Cannon-Ubbelohde viscometer at 25 °C. The reduced viscosities ranged between 1.26 and 1.88.

Results

Influence of temperature

The conversions of NIPAM and BA were measured and are shown as functions of reaction time

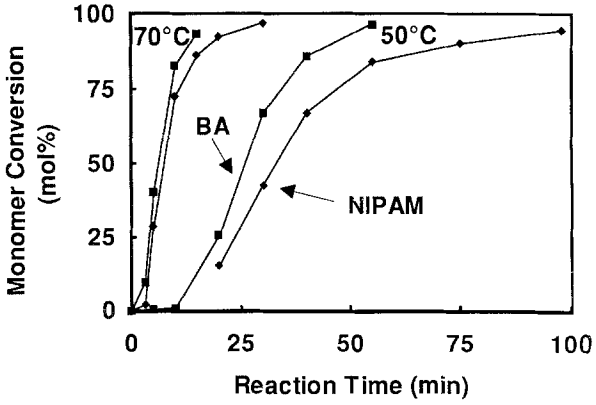

Fig. 1. BA ■ and NIPAM ◆ conversion as function of reaction time for LS1 (70 °C) and LS6 (50 °C).

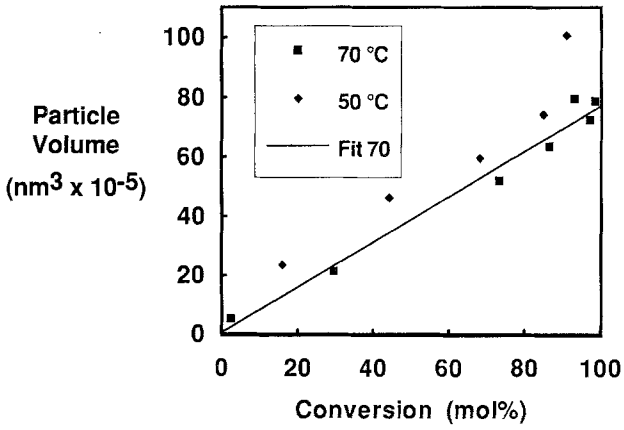

Fig. 3. Average microgel particle volume as function of conversion for LS1 (70 °C) and LS6 (50 °C).

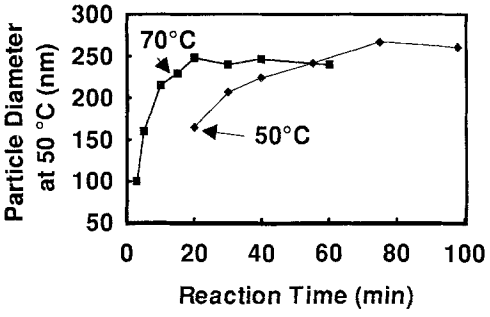

Fig. 2. The influence of polymerization temperatures on the volume average particle diameters measured at 50 °C as functions of reaction time. Data for microgel latexes LS1 (70 °C) and LS6 (50 °C).

in Fig. 1. Induction periods were observed at both temperatures. We believe that these were due to the presence of trace quantities of oxygen. At both 50° and 70 °C BA was consumed more quickly than was the NIPAM. At 70 °C the polymerization gave high yields at less than 50 min whereas at 50 °C there remained unreacted NIPAM monomer 100 min after addition of the initiator. The initial reaction rates were 1.9 mol/L min. at 70 °C and 0.36 mol/L min. at 50 °C. Assuming the rate constants obey the Arrhenius equation, the overall activation energy calculated from the two rates is 18 kcal/mol which is close to the value of 17.8 kcal/mol determined for acrylamide [7]. Particle diameters of samples taken during the polymerization were measured by dynamic light scattering at 50 °C. The average diameters are shown as functions of reaction time in Fig. 2. The higher temperature latex grew more quickly, however, the final particle diameter at 70 °C was about 10% lower than the 50 °C preparation.

Since for both polymerizations the initial monomer concentrations were the same and the final conversions were high, the final particle diameters reflect the relative concentration of particles. Specifically, the higher temperature preparation produced more latex particles. Similar effects have been observed for the surfactant-free polystyrene latex formed by homogeneous nucleation [8].

Figure 3 shows the average particle volumes calculated from the diameters, versus the mol percentage total conversion. The solid line is the least squares fit through the higher temperature data. Results from both temperatures were approximately linear to 85% conversion above which the volumes showed a positive deviation. Linear curves imply that: all the polymer ends up in the particles; the particle concentration was constant over the conversion range studied, and, that the degree of swelling was independent of conversion.

Influence of BA

Our previous work has shown that the diameter of polyNIPAM latex increased with BA concentration, however, too much BA led to colloidally unstable particles [4]. Figure 4 compares total monomer conversion versus time curves with and without BA at 70 °C and the particle diameters are shown in Fig. 5. Estimates

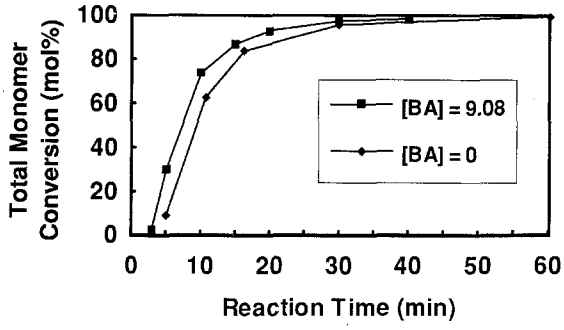

Fig. 4. Influence of BA concentration on conversion time curves for LS1 (Initial [BA] = 9.08 mmol/L) and LS8 (initial [BA] = 0 mmol/L).

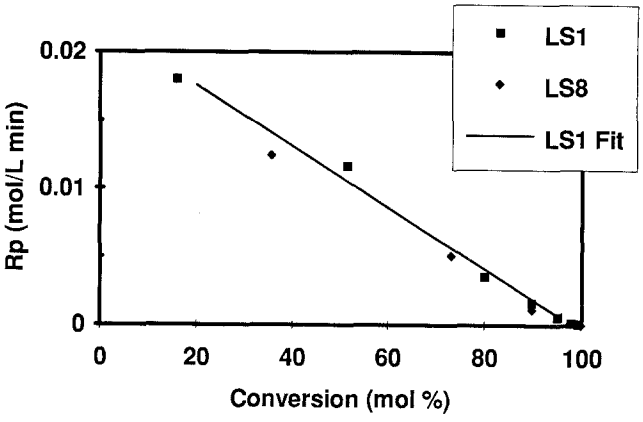

Fig. 6. The influence of initial BA concentration (mmol/L) on rates of polymerization. Solid line is least squares fit of LS1 data excluding first point.

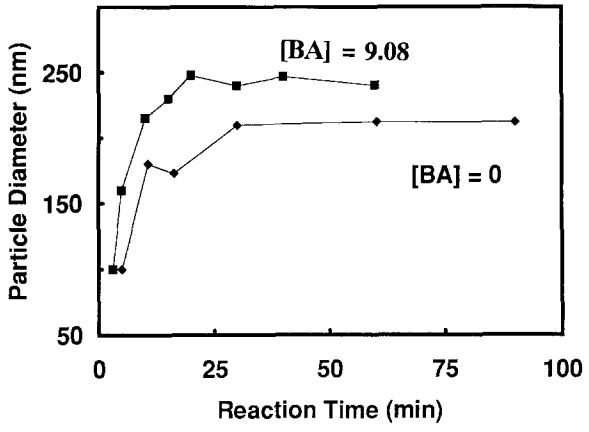

Fig. 5. Volume average particle diameter, measured at 50 °C, versus reaction time for LS1 and LS8. The LS8 samples temperatures were never allowed to go below 50 °C to ensure that the particles did not dissolve.

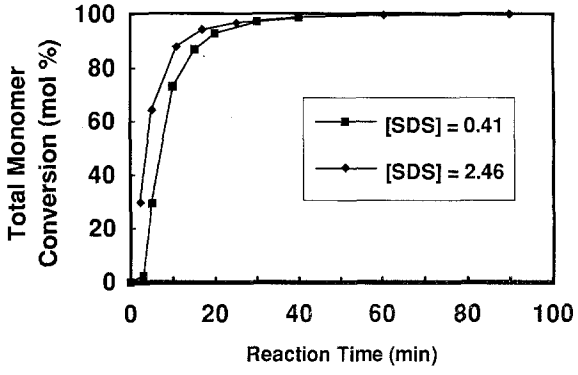

Fig. 7. Influence of SDS concentration (mmol/L) in polymerization on the reaction rate of copolymerization of NIPAM and BA (LS1 and LS10).

of reaction rate were made based on the slope of total monomer conversion versus time curves and the results are shown in Fig. 6. The two sets of data appear to fall on the same straight line, indicating that BA did not have a large effect on the course of the polymerization. After the induction period the reaction rate decreased with conversion, suggesting that there was no evidence for rate enhancement due to gel effect.

Influence of SDS concentration

McPhee et al. showed that the average diameter of polyNIPAM latex decreased with increasing SDS concentration, which indicated that SDS participated in particle nucleation [4]. The effects of SDS on conversion and reaction rate are shown in Fig. 7. Both SDS concentrations were below the critical micelle concentration of SDS in water. Reaction rate versus conversion plots are shown in Fig. 8. Except for the duration of the induction period, the reaction rate profiles were not sensitive to the SDS concentration. The corresponding diameter data are shown in Fig. 9. Confirming previous work, the higher SDS concentration gave lower particle diameters. Thus, polymerization rates do not seem sensitive to particle size.

Six polymerizations were done at six different SDS concentrations and the final particle diameters of polyNIPAM microgel latexes are shown

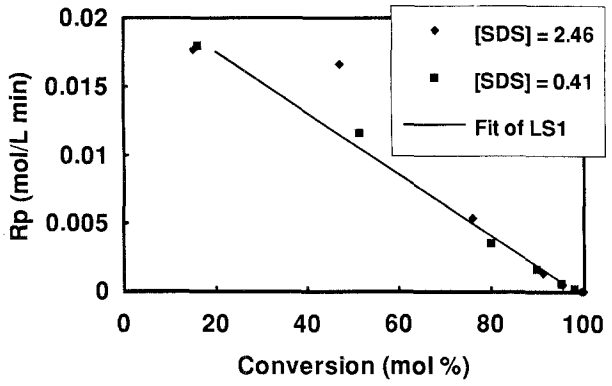

Fig. 8. Influence of SDS concentration on reaction rate versus conversion curves for latexes LS1 and LS10.

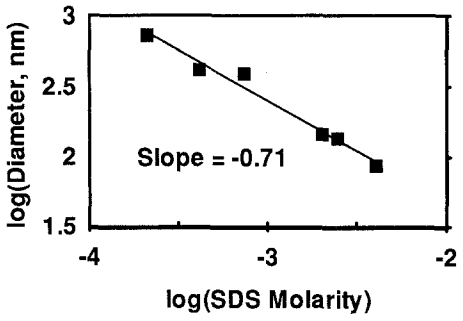

Fig. 10. Volume average particle diameters, determined at 50 °C, as a function of the SDS concentration used to prepare the latex. Latexes: LS1, LS10, 5-76, 5-72, 5-70, and 5-75.

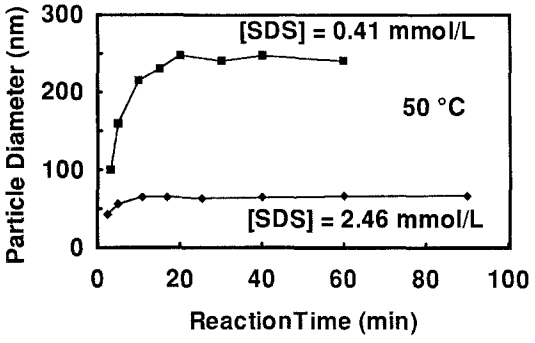

Fig. 9. Influence of SDS concentration on volume average particle diameters measured at 50 °C particle diameter versus reaction time (LS1 and LS10).

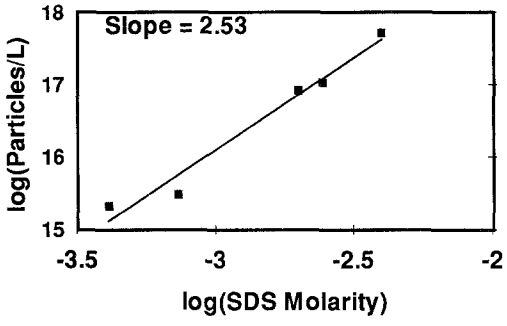

Fig. 11. Influence of SDS on the concentration of polyNIPAM latex particles for latex LS1, 5-70, 5-72, 5-76, and LS10.

as functions of the SDS concentrations in Fig. 10. The fitted line on the double logarithmic plot predicts $D \propto [\mathrm{SDS}]^{-0.71}$ where D is diameter.

Previous work has shown that at 50 °C a polyNIPAM microgel latex contained about 10 weight percent water. Water swelling means that the number concentration of latex particles in the final latex cannot be simply calculated from the weight concentration of polyNIPAM and the particle size distribution. In this work, latex particle concentrations were estimated from viscosity data combined with particle diameters (see experimental section). Figure 11 shows the number concentration of latex particles as functions of the SDS concentrations. The data were approximately linear on double log plot with a slope of about 2.5. The absence of an inflection point suggests that there was no change in nucleation mechanism in the range of SDS concentrations studied. This high exponent is more characteristic of homogeneous nucleation with unity being an upper limit for micellar nucleation.

Development of latex properties

a) Average latex properties

Figure 12 shows intensity and volume average diameters, from dynamic light scattering, for two polyNIPAM latexes as a function of temperature. The volume averages were greater and the differences between the two averages, which is a measure of the width of the particle size distribution, were greatest when the particles were swollen. Above 50 °C the particle size is constant.

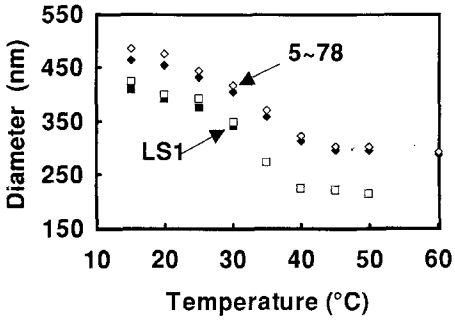

Fig. 12. Average particle diameters versus temperature for latexes LS1 and 5–78. Solid points are intensity averaged whereas open points are volume averaged. For LS1 the standard deviations ranged between 10 and 18% of the mean.

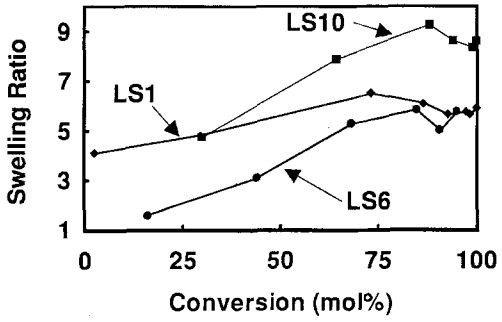

Fig. 13. Influence of conversion on polyNIPAM latex microgel swelling for latexes LS1, LS6, and LS10. The swelling ratio is defined as the volume at 25 °C divided by the volume at 50 °C. Volumes were calculated from the volume averaged diameters measured by DLS.

Therefore, the ratio of particle volume at 25° to those at 50 °C gives a measure of the swelling capacity of the latex, which in turn is a reflection of the crosslink density.

The extent of polyNIPAM swelling in water was determined by measuring the swelling ratio defined as the average volume at 25 °C divided by the volume at 50 °C. Average volumes came from dynamic light scattering measurements. Shown in Fig. 13 are swelling ratios as a function of monomer conversion. For all three latexes swelling increased with conversion up to a maximum between 75 and 90% conversion, after which there was a slight drop in swelling. Presumably, the drop in swelling was due to increased crosslinking as pendant double bonds (from the BA) were consumed. As expected, latex swelling decreased

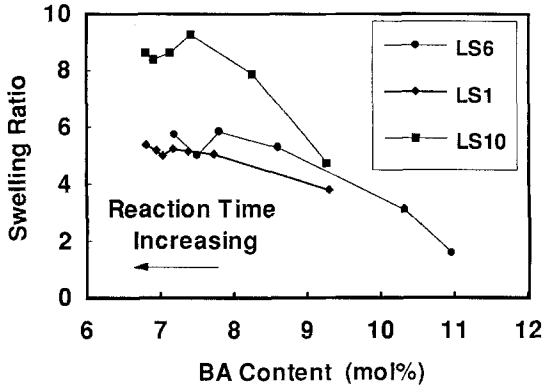

Fig. 14. Swelling ability of polyNIPAM latexes as a function of the BA content determined from residual monomer concentrations. The initial BA contents restricted swelling compared with the later stages in the polymerizations.

with increased BA concentration in the polymerization recipe.

Combining swelling versus time data with conversion data gives swelling ratio as a function of the BA in the particles. Figure 14 shows such a plot for three latexes. In all cases the average BA content of the particles decreased with increasing conversion or reaction time because the BA was consumed more quickly than NIPAM. As before, the ability of the latexes to swell with water increased with decreasing average BA content in the particles. Latexes LS1 and LS6 roughly fell on the same curve, indicating that the swelling was dictated by the BA content irrespective of polymerization temperature. By contrast, LS10, which was made with more SDS, showed more swelling.

The role of BA was to prevent the polyNIPAM particles from dissolving when the latexes were cooled below the CPT. The need for BA was illustrated by the following experiments. Samples from preparations LS1 and LS8 (no BA) were taken during the polymerization. The samples were split: the diameters of one set were determined at 50 °C by DLS without allowing the latexes to cool. The second set was allowed to cool to room temperature and was re-heated to 50 °C for DLS. Figure 15 shows for each sample the diameter obtained after cooling and re-heating versus the never-cooled diameter. For LS1, with BA, the diameters were independent of thermal history whereas for LS8, the re-heated diameters were lower. Therefore upon cooling LS8 dissolved and upon re-heating new smaller particles formed.

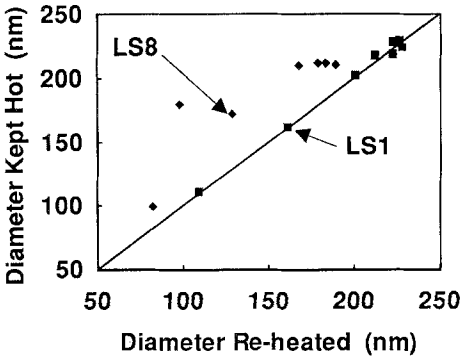

Fig. 15. Volume average diameters of poly NIPAM latexes LS1 and LS8 at 50 °C. Diameters measured for samples which were not allowed to cool plotted against the diameters obtained after the samples were allowed to cool to room temperature and then were re-heated to 50 °C. With BA there was no effect of temperature history. Without BA the particles dissolved when cooled and precipitated when re-heated to give a different diameter.

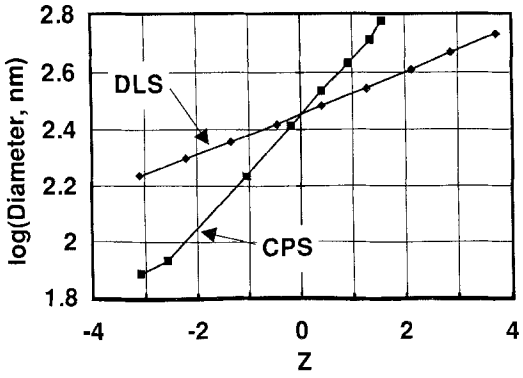

Fig. 16. Particle size distributions of latex LS1 in acetonitrile at 25 °C determined by dynamic light scattering, DLS, and by a centrifugal particle sizer, CPS. The data are plotted on a log/probability plot. The Z values (quartiles) are the inverse of the experimental cumulative probabilities. The CPS raw data were scaled to give the same mean as the DLS by assigning an average density of the swollen polyNIPAM to equal 0.889 g/mL. The slope of the CPS curve was greater indicating a broader apparent particle size distribution.

b) Property distributions

The particle size distribution of LS1 in acetonitrile was measured with a Horiba CAPA 700 centrifugal particle size measurement apparatus – herein called CPS. With the CPS instrument, a uniform suspension is placed in a glass cell mounted on a spinning disk. Particle migration in the centrifugal field is measured by a turbidity sensor at a fixed location in the cell. For constant velocity operation, $D(t)$ the particle diameter measured at sedimentation time t is given by the following expression where K is an instrument constant and $\Delta\rho$ is the density difference between the solvent and the solvent swollen particle (assumed to be a solid sphere).

$$D(t)^2 \Delta\rho = \frac{K}{t} \tag{3}$$

In conventional operation of the CPS, the densities of the solvent and particles are known and the instrument measures a particle size distribution. The density of the polyNIPAM microgel particles was not accurately known. However, if it was assumed that the density of all the particles equaled 0.889 g/mL, the mean diameter from the CPS equaled that from dynamic light scattering.

An approach to evaluating how closely experimental size versus cumulative probability data follows a log normal distribution is to plot the data on log probability paper. A perfect fit yields a straight line with a slope equal to the standard deviation of the log normal distribution. With spreadsheet programs, log probability plots are obtained by plotting the logarithm of experimental diameters versus corresponding Z values (sometimes called quartiles) where Z is the inverse of the normal cumulative probability. Figure 16 shows the log of the particle diameter versus Z for both the DLS and CPS data. The distribution from the CPS was nearly linear, indicating a log normal distribution, however, the standard deviation of the distribution was much higher for the CPS data than that from the DLS results. Note that the two curves coincided at $Z = 0$ (corresponding to the average diameter) because the average density of the particles in the CPS data was chosen to give this result. Assuming a different value for the average density of the particles shifted the CPS curve horizontally but did not alter the slope, which is a measure of the width of the distribution.

The obvious explanation for the observation that the standard deviation from CPS was much greater than that determined by DLS is that the instruments were not sufficiently accurate for the results to coincide. However, another explanation is possible. In addition to a distribution of particle sizes it is reasonable to expect that polyNIPAM microgel latexes also have a distribution

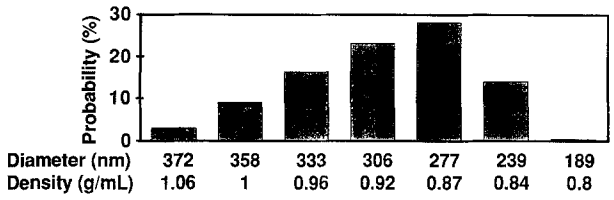

Fig. 17. Estimated density distribution for latex LS1 in acetonitrile based upon assumption that differences between particle size distributions measured by DLS and CPS can be explained by density variations. Diameters were from DLS.

of densities or equivalently a distribution of degrees of swelling, both being a result of a distribution of BA contents. An estimate of the density distribution for latex LS1 was made by the following procedure. First, it was assumed that the particle diameter distribution given by dynamic light scattering was correct. Second, it was assumed that the additional breadth of the CPS size distribution in Fig. 16 was due to a distribution of densities. Thus, for each bin in the CPS generated particle size distribution the corrected density difference, $\Delta\rho_c$, was calculated from the following equation which comes from Eq. (3) where D_c is the corrected diameter and D_a is the apparent diameter given by the CPS instrument for an assumed value of $\Delta\rho$.

$$D_a^2 \, \Delta\rho = D_c^2 \, \Delta\rho_c \tag{4}$$

To summarize, a value of $\Delta\rho$ was assumed for the CPS experiment which produced a set of D_a values along with the corresponding cumulative probabilities. The fit of the DLS data in Fig. 16 was used to calculate D_c values for each cumulative probability. Finally, Eq. (4) was used to give the corresponding set of $\Delta\rho_c$ values. Apparent particle densities were obtained by subtracting the density of acetonitrile from $\Delta\rho_c$. Figure 17 shows the calculated density distribution along diameters interpolated from the DLS data. On the basis of the above assumptions there was a large distribution of densities and the highest densities corresponded to the largest particles.

Discussion

The polyNIPAM system offers both advantages and complications. An advantage is that particle diameters can be determined easily as a function of swelling by dynamic light scattering at different temperatures near the CPT. In earlier work it was shown that these measurements permit experimental estimation of effective crosslink density if χ, the Flory Huggins interaction parameter, is known or estimation of χ if the crosslink density is assumed. On the other hand, water swelling of the particles during polymerization makes it difficult to determine accurately the number concentration of latex particles as a function of polymerization time or conversion. This situation can be illustrated by comparing two methods for estimating the final particle concentration of LS1.

The analysis of the CPS data summarized in Fig. 16 led to the conclusion that the average density of LS1 swollen with acetonitrile was 0.889 g/mL. The partial specific volume of polyNIPAM-co-BA was assumed to be 1.07 g/mL, the value in the literature for amorphous polyNIPAM [9, 10]. The average weight of copolymer per LS1 microgel particle was calculated from the swollen particle density and the number concentration of latex came from the mass balance to give a value of 2.9×10^{15} particles/L. By comparison the viscosity method (from Eqs. (1) and (2) gave a value of 2.1×10^{15} particles/L. Both methods are sensitive to the cube of the average diameter, which is perhaps the largest source of error. For future work perhaps the best estimates of particle concentrations would come from diameters measured at 50 °C together with a measurement of particle density at that temperature – our CPS apparatus does not have temperature control for high temperature operation. The advantage of determinations at 50 °C is that the particles contain little (ca. 10%/wt) water which should increase both the accuracy of the DLS (because the particles are smaller) and the density determination (because of increased density difference between the particles and water).

Nucleation

PolyNIPAM is not soluble at the polymerization temperature. Phase separation studies with linear polymer suggest that the LCST was not sensitive to molecular weight. Indeed, small molecule studies suggest that oligomers with only three repeat units will phase separate [11]. For

these reasons, we believe that locus of polymerization is in phase separated polymer particles. It seems logical that the small initially formed particles (i.e., precursor particles in the nomenclature of Napper and coworkers [12]) were colloidally unstable. Therefore, the nucleation of colloidally stable particles will be from the coagulative association of precursor particles. All the work in this paper involves the use of SDS; however, we have shown that polyNIPAM microgel latexes can be made without surfactant [3]. All experiments were conducted at SDS concentrations below the critical micelle concentration so micellar nucleation is not possible. On the other hand, work in this and other laboratories (see refs. contained in [13]) have shown that above concentrations of 0.7 mmol/L at 25 °C SDS associates with aqueous polyNIPAM homopolymer. The interaction of SDS with polyNIPAM at the temperatures used in the polymerizations (50 to 70 °C) has not been studied because of the difficulty in making measurement with phase separated polymer. Nevertheless, it seems reasonable to assume that since polyNIPAM is less hydrophilic above the CPT it would be favorable for SDS to adsorb onto the surface of phase separated polyNIPAM particles. In summary, we believe that polyNIPAM microgel latex particles form by homogeneous nucleation. Furthermore, the role of SDS in particle nucleation is to increase the colloidal stability of precursor particles and thus lower the diameter of primary particles.

Figures 3 showed that the particle volumes were linear with conversion. This implies that for most of the polymerization the number concentration was constant. In other words, the particle nucleation stopped at low conversions. Further support for a rapid nucleation process was the fact that the particle size distributions, as determined by dynamic light scattering, were narrow; typically σ values ranged from 15 to 20% of the mean diameter.

Propagation

In classical emulsion polymerization following Case II kinetics ($\bar{n} = \frac{1}{2}$) the rate of polymerization is proportional to the number concentration of latex particles. A remarkable feature of the polyNIPAM polymerizations was that the polymerization rate was not sensitive to particle number concentration. For example, the conversion curves shown in Figs. 7 and 8 were roughly equal, whereas the corresponding final latex particle concentrations were 2×10^{15} particles per liter for the lower SDS concentration compared with 1×10^{17} for the higher. For systems which obey Case I kinetics ($\bar{n}$ decreases with decreased polymer particle size or increased particle concentration). The product $\bar{n}N_p$ may therefore be almost independent of particle size.

Table 2. Comparison of LS1 and LS10. The maximum rate came from experimental conversion measurements. The volume fraction of particles, ϕ, was estimated by multiplying Np times the average particle volume at the point of maximum conversion.

	LS1	LS10
Rp max, mol/L min	0.0180	0.0177
Np, m^{-3}	2×10^{18}	1×10^{20}
ϕ	0.0027	0.0039

Barrett gives an expression for the rate of polymerization in dispersion polymerization in which the rate is proportional to the square root of the volume fraction of particles [14]. The same equation corresponds to Smith Ewart Case III kinetics which applies for the case of many radicals per particle.

The experimentally determined maximum rates of polymerization for LS1 and LS10 are given in Table 2 together with the number concentration of latex particles and an estimate of the volume fraction of particles corresponding to maximum rate. The volume fractions were estimated by multiplying the final particle concentration by the average volume per particle calculated from the particle size data. The maximum rates for the two polymerizations were nearly the same as were the volume fractions of particles. Therefore, the present data does not discount the contention that the rate of polymerization is proportional to the square root of the volume fraction of particles. Much more data would be required in order to develop detailed kinetic relationships.

polyNIPAM microgel latex morphology

The analysis of CPS data relative to the DLS results (Figs. 16 and 17) suggested that the larger particles were less swollen with acetonitrile than

were the smaller ones, which in turn implies that the larger particles were characterized by a larger average BA content. If the larger particles were nucleated first, this conclusion is consistent with the kinetic results which showed that the first polymer formed contained more BA than did the polymer formed at the end of the polymerization. This implies that the crosslink density of the first formed polymer will be higher. It is emphasized that the analysis leading to Figs. 16 and 17 was speculative because it required the results of DLS and CPS to be correct and directly comparable.

Swelling measurements have been used traditionally to characterize crosslinking. In this work we presented swelling ratio data which are particle volumes at 25 °C divided by the particle volume at 50 °C. At 25 °C the particle volume is sensitive to amount of crosslinking, whereas at 50 °C the water content is low and should not be very sensitive to small changes in the concentration of BA in the particle. Therefore, the swelling ratio is a good estimate of the absolute degree of swelling at 25 °C.

The development of crosslinking within a particle in the course of the polymerization is illustrated in Fig. 13 which shows that swelling ratio increased with conversion except for a possible slight decrease at the end of the polymerization. It is emphasized that the changes in swelling shown in Fig. 13 are large. For example, for LS10 the swelling ratio at the end of the reaction was 1.5 times greater than the value at 30% conversion. The obvious explanation is that the first polymer formed was rich in BA which limited swelling, whereas the last polymer formed within a particle was much less crosslinked. This argument suggests that within the particles there may highly crosslinked domains within a less crosslinked matrix.

Another interesting feature of Fig. 13 is that the three latexes had the same BA content, however, LS10 exhibited much more swelling with water at 25 °C at the end of the polymerization. LS10 was made with a higher concentration of SDS, perhaps indicating that the surfactant influenced the distribution of BA within the particles.

In summary, kinetic results combined with particle size and sedimentation data suggest that the polyNIPAM microgel latexes have domains of higher crosslinking within the particles. Furthermore, the ability of the particles to swell was less for the larger particles, giving a swelling distribution between particles. These conclusions were possible because of the ability to measure the swelling ratio by dynamic light scattering. Crosslinking distributions within and between particles could also occur in other crosslinked latex systems where swelling ratio measurements are not as facile.

Conclusions

1) PolyNIPAM microgel polymerizations in water were rapid at 50° and 70 °C. High conversions were obtained within the first hour.
2) Microgel particle formation was by homogeneous nucleation. SDS served to help colloidally stabilize the primary particles.
3) The number concentration of latex particles increased with SDS concentration.
4) Initial indications are that polymerization kinetics followed Smith Ewart Case III kinetics or, equivalently, the case of dispersion polymerization where polymerization occurs only in the particles and the average number of radicals per particle is greater than one.
5) Latex number concentrations can be estimated by methods based on viscosity or centrifugal particle size data. Both treatments require accurate particle size measurements from dynamic light scattering.
6) There is evidence of significant variations of crosslink density within the microgel particles. Furthermore, the average crosslink density appeared to be higher for the larger particles within a latex sample.

Acknowledgements

This work was supported by the Canadian Natural Science and Engineering Research Council.

References

1. Schild HG (1992) Prog Polym Sci 17:163
2. Pelton RH, Chibante P (1986) Colloids and Surfaces 20:247
3. Pelton RH, Pelton HM, Morfesis A, Rowell RL (1989) Langmuir 5:816
4. McPhee W, Tam KC, Pelton RH (1993) J Colloid Interface Sci 156:24

5. Kawaguchi H, Fujimoto K, Mizuhara Y (1992) Colloid and Polymer Sci 270:53
6. Thomas DG (1965) J Colloid Sci 20:267
7. Thomson RAM, Ong CK, Rosser CM, Holt JM (1983) Makromol Chem 184:1885
8. Goodwin JW, Hearn J, Ho CC, Ottewill RH (1974) Br Polym J 5:347
9. Sewell JH (1973) J Appl Polym Sci 17:1714
10. Chiklis CK, Grasshoff JM (1970) J Polym Sci, Part A2 8:1617
11. Snyder WD, Klotz IM (1975) J Amer Chem Soc 97(17): 4999
12. Feeney PJ, Napper DH, Gilbert RG (1987) Macromolecules 20:2922
13. Wu XY, Pelton RH, Tam KC, Woods DR, Hamielec AE (1993) J Polymer Sci Part A 31:957
14. Barrett KEJ (1975) Dispersion Polymerization in Organic Media. John Wiley & Sons, London

Received October 30, 1992;
accepted May 13, 1993

Authors' address:

Prof. R.H. Pelton
McMaster Centre for Pulp and Paper Research
Dept of Chemical Engineering
JHE-136
McMaster University
Hamilton, Ontario
Canada L8S 4L7